results could be useful for drilling, and we suggest that such an approach should be routinely applied to seismic data before drilling. If many BSRs are underlain by gas, methane must be present in sufficient concentrations to exceed its solubility at ocean bottom pressures. Such concentrations are not readily attained by in situ biogenic degradation of organic material (25). They may be attained by upwelling of free or dissolved methane generated at depth or, alternatively, by thermal perturbations such as those caused by continued sedimentation, which cause the base of the zone of hydrate stability to rise through the sediment column.

Although the insensitivity of velocity to gas saturation above ~1% does not allow tight constraints to be placed on the degree of gas saturation beneath the BSR, we can be confident that gas is present and can estimate the thickness of the gaseous zone (about 30 m in the areas we have studied). We can also estimate the quantity of hydrate present immediately above the BSR—at the VI-5 site it appears to be small because the velocity increase is at most ~5% above the background velocity (Fig. 4A), which corresponds to a hydrate saturation of only ~10%. The drilling results from site VI-5 will provide a direct test of these estimates and allow the relation between the seismic velocity and degree of gas or hydrate saturation to be investigated in detail.

The amount of carbon stored in and beneath gas hydrates may exceed that in all fossil fuel deposits (5). BSRs have been identified in at least 22 continental margin locations worldwide, and multichannel seismic reflection data have been acquired at many of these locations. As computers become faster and techniques are refined, one- and two-dimensional inversion schemes should routinely be applied to large multichannel data sets and ultimately should be able to put well-constrained quantitative limits on the global methane resource stored immediately above and below the BSR.

## REFERENCES AND NOTES


1. K. A. Kvenvolden and L. A. Barnard, *Am. Assoc. Petrol. Geol. Mem.* **34**, 631 (1982).
2. M. Yamano, S. Uyeda, A. Y. Aoki, T. H. Shipley, *Geology* **10**, 339 (1982).
3. R. D. Hyndman *et al.*, *Earth Planet. Sci. Lett.* **109**, 289 (1992).
4. D. J. Milton, in *The Future Supply of Nature-Made Gas Technical Reports*, R. F. Meyer, Ed. (Pergamon, New York, 1976), pp. 927–943.
5. K. A. Kvenvolden, *Chem. Geol.* **71**, 41 (1988).
6. T. J. McDonald, *Clim. Change* **16**, 247 (1990).
7. T. A. Minshull and R. S. White, *J. Geophys. Res.* **94**, 7387 (1989).
8. J. J. Miller, M. W. Lee, R. von Huene, *Am. Assoc. Petrol. Geol. Bull.* **75**, 910 (1991).
9. R. D. Hyndman and G. D. Spence, *J. Geophys. Res.* **97**, 6683 (1992).
10. G. D. Spence, R. D. Hyndman, E. E. Davis, C. J. Yorath, in *Continental Lithosphere: Deep Seismic Reflections*, R. Meissner *et al.*, Eds. (*Geodynamics Series*, vol. 22, American Geophysical Union, Washington, DC, 1991), pp. 257–263.
11. E. E. Davis, R. D. Hyndman, H. Villinger, *J. Geophys. Res.* **95**, 8869 (1990).
12. P. W. Cary and C. H. Chapman, *Geophys. J. Int.* **93**, 527 (1988).
13. S. C. Singh, M. Dietrich, F. Chapel, in (*10*), pp. 391–400.
14. Slowness is given by $(\sin\theta)/v$, where $\theta$ is the angle of incidence at the surface and $v$ is the seismic velocity at the surface.
15. F. Kormendi and M. Dietrich, *Geophysics* **56**, 665 (1991).
16. We used CMPs 3109 to 3112 from the line 89-08, combined into a 144-fold composite CMP gather. A CMP gather is a set of seismic recordings in which the distance between the source and receiver varies about a fixed midpoint. The CMP data set has a trace spacing of 25 m. The transformation to slowness was achieved with the exact formulation of Chapman (*26*). Slownesses of 0.01 to 0.50 s/km were sampled at an interval of 0.01 s/km, and the time sample interval was 8 ms.
17. E. Landa, P. Thore, V. Sorin, Z. Koren, *Geophysics* **56**, 1377 (1991).
18. B. Andressen *et al.*, *J. Phys.* **49**, 1485 (1988).
19. B. L. N. Kennett and N. J. Kerry, *Geophys. J. R. Astron. Soc.* **57**, 557 (1979).
20. E. L. Hamilton, *Geophysics* **41**, 985 (1976).
21. W. F. Murphy, *J. Geophys. Res.* **89**, 549 (1984).
22. E. L. Hamilton, *J. Acoust. Soc. Am.* **634**, 366 (1978).
23. During each run, we scaled the synthetic seismograms so that the amplitude ratio of data and synthetic seismograms at the seabed was the same as that for the starting model. This required changes up to 20% in the scaling factor because different bandwidths were used in successive runs and because the seabed reflection coefficient depended on the frequency in both the data and synthetic seismograms. In each run, 161 velocity parameters were inverted. The top layer, 1.152 km thick, was assumed to be water with a velocity of 1.477 km/s, and the rest of the layers were each 8 m thick. Starting from the inverted velocity model of the previous runs, we performed five iterations of inversion in each run.
24. T. A. Minshull, S. C. Singh, G. K. Westbrook, *Ann. Geophysicae* **10** (suppl. 1), C92 (1992).
25. R. D. Hyndman and E. E. Davis, *J. Geophys. Res.* **97**, 7025 (1992).
26. C. H. Chapman, *Geophys. J. R. Astron. Soc.* **66**, 445 (1981).


30 November 1992; accepted 2 February 1993

# Impairment of V(D)J Recombination in Double-Strand Break Repair Mutants

Guillermo E. Taccioli, Gary Rathbun, Eugene Oltz, Thomas Stamato, Penny A. Jeggo, Frederick W. Alt

**Cells maintain the integrity of their genome through an intricate network of repair systems that recognize and remove lesions from DNA. The only known site-directed recombination process in vertebrates is the V(D)J recombination of lymphocyte antigen receptor genes. A large panel of cell lines deficient in DNA repair were tested for the ability to perform V(D)J recombination after introduction of the *RAG-1* and *RAG-2* genes. Two mutants failed to generate normal V(D)J recombination, and further analysis provided evidence for two distinct nonlymphoid-specific genes that encode factors involved in both DNA repair and V(D)J recombination.**

V(D)J recombination is a complex reaction that likely involves numerous activities. These include recognition of conserved heptamer-spacer-nonamer sequences (RS sequences) that flank germline V, D, or J segments, introduction of site-specific double-strand breaks between the elements to be joined and the RS sequences, potential deletion, with or without addition of nucleotides, at coding junctions, and polymerization and ligation activities [(*1*) and Fig. 1, A to C]. The differential processing of the coding and RS joins is an unusual aspect of V(D)J recombination. Nucleotides are frequently lost from the former but not the latter.

G. E. Taccioli, G. Rathbun, E. Oltz, F. W. Alt, Howard Hughes Medical Institute, Children's Hospital, and Department of Genetics, Harvard University Medical School, Boston, MA 02115.
T. Stamato, Lankenau Medical Research Center, Wynnewood, PA 19096.
P. A. Jeggo, Medical Research Council Cell Mutation Unit, University of Sussex, Brighton, United Kingdom BN1 9RR.

Two genes, recombination activation genes 1 and 2 (*RAG-1* and *RAG-2*), have been identified that, when expressed simultaneously in a nonlymphoid mammalian cell, generate V(D)J recombinase activity (*2*). The *RAG* genes either encode or activate the tissue-specific activities necessary for initiation of V(D)J recombination (*1*). By analogy to site-specific recombination systems of yeast and bacteria, the specific components of V(D)J recombinase may recruit ubiquitously expressed cellular activities to perform certain aspects of the reaction. One such activity may be encoded by the gene affected by the mouse severe combined immune deficient (SCID) mutation (*3*); homozygous *scid* mutants are impaired in one of the terminal steps of V(D)J recombination (*4*) and also have a defect in double-strand DNA break repair (DSBR) in lymphoid and nonlymphoid cells (*5*).

To test whether or not DNA repair processes and V(D)J recombination share common factors, we assayed a number of

mutant Chinese hamster ovary (CHO) cell lines defective in different pathways of DNA repair for the ability to rearrange introduced V(D)J recombination substrates. Cells were transiently transfected with RAG expression vectors driven by a long terminal repeat (LTR) promoter providing the specific V(D)J recombination functions to the nonlymphoid cells and, simultaneously, with extrachromosomal V(D)J recombination substrates that, when recovered and assayed in bacterial cells, permit evaluation of the approximate level and fidelity of V(D)J recombination (*6*). Two different substrates were used; one (pJH290) allows recovery of coding joins, whereas the other (pJH200) allows recovery of RS joins (*7*). In each case, V(D)J recombination activity was estimated by the relative amount of rearranged substrate (based on gain of chloramphenicol resistance, $Cam^R$) as compared with the total amount of recovered substrate (based on generation of ampicillin resistance, $Amp^R$) (Table 1).

None of the cell lines examined possessed measurable V(D)J recombination activity in the absence of cotransfected RAG vectors (Table 1; mock transfectants); the integrity of the recovered substrates confirmed that deletions do not appear in the absence of RAG expression. As expected, introduction of RAG vectors generated V(D)J recombination activity in all wild-type lines at a level consistent with that seen by others using this assay (*2*) (Table 1). Seven ultraviolet (UV) light–sensitive mutants that belong to independent complementation groups (*8*), most deficient in excision repair, were tested and all had levels of V(D)J recombination activity similar to that of wild-type lines (Table 1). We tested five independent x-ray–sensitive mutants, four of which are defective in DSBR (*9*, *10*). Of these mutants, two (xrs-6 and XR-1) showed blocks in the ability to form both coding and RS joins (Table 1).

In addition to the defect in DSBR, the xrs-6 and XR-1 lines share a similar spectrum of sensitivity to ionizing radiation, radiomimetic drugs, and alkylating agents (*9*). However, complementation studies using cell fusion showed that these mutants belong to different complementation groups [(*9*) and Table 1]. In support of this finding, correction of the radiosensitive phenotype of xrs-6 could be attained by the introduction of human chromosome 2 (*11*) and that of XR-1 by the introduction of human chromosome 5 (*12*). Both the XR-1 and xrs-6 lines, after complementation by human chromosomes, as well as an independent xrs-6 reactivant (*9*), also regained normal levels of V(D)J recombination activity (Table 1). The simultaneous correction of both the ionizing radiation sensitivity and the V(D)J recombination defects by specific chromosomal segments provides strong evidence that these two processes share common gene products.

To characterize further the V(D)J recombination defect in the CHO mutants, we analyzed the structure of RS joins and coding joins recovered from xrs-6 and XR-1 transfectants. Analysis of restriction endonuclease digestions of polymerase chain reaction (PCR) products of pJH200 substrates recovered from each mutant indicated that more than 80% of the RS joins were imprecise, with deleted nucleotides from one or both RS sequence (Table 1 and Fig. 2). This contrasts to the fidelity of joins from wild-type cells, revertants, or from other

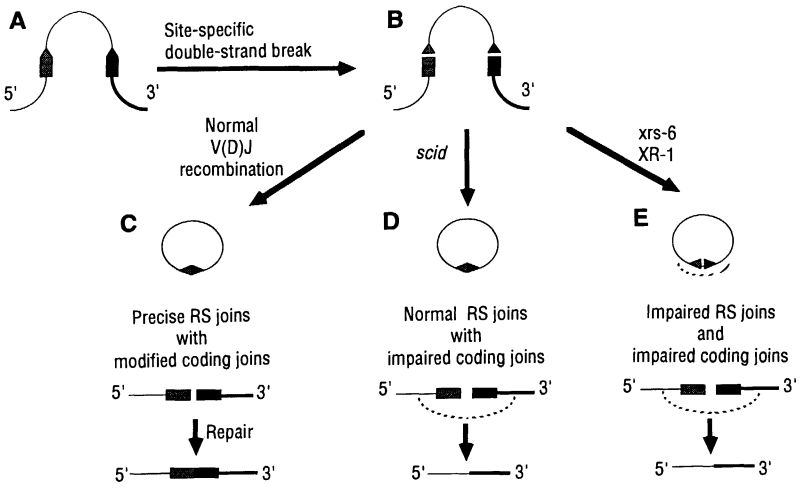


**Fig. 1.** Impact of mutations on V(D)J recombination. (A to C) Normal pathway of V(D)J recombination (*1*). (**A**) RS elements are indicated by triangles, and coding sequences are indicated by boxes. (**B**) During normal V(D)J recombination, double-strand breaks are introduced between the RS and adjacent coding sequences. (**C**) Generation of precise RS joins and trimmed coding joins. (**D**) Defective joining in *scid* mutants. Double-strand breaks appear to be properly introduced in *scid* cells, RS joins occur relatively normally, but coding joins are impaired. (**E**) Defective joining in xrs-6 or XR-1 cells. Double-strand breaks occur normally, but both RS and coding sequence joining is impaired.

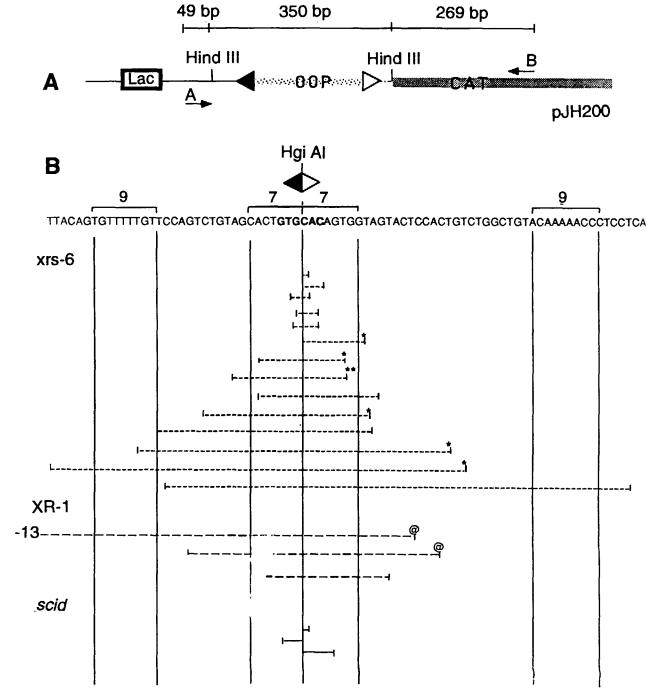


**Fig. 2.** Nucleotide sequence of selected RS joins. (**A**) Map of the pJH200 (*6*) region that contains the RS sequences. The box represents the lactose promoter (Lac) from which the CAT gene is expressed after the transcription terminator (OOP) is eliminated by recombination involving RS (triangles) joins (*6*). The location of primers used to generate PCR products for analysis of RS joins is indicated by arrows (*22*). (**B**) The sequence shown is the product of two signal ends fused without base loss after V(D)J recombination. The site for the restriction enzyme Hgi AI (indicated in bold) is generated only after precise fusion of heptamers (*6*). The bracketed dashes show the extent of the deletions in substrates recovered from the various lines (indicated at the left). The deletions shown were selected and are not representative of the overall size distribution (text). Asterisks and @ represent bases that cannot be unequivocally assigned in each group.

DNA repair mutants in which levels of V(D)J recombination were not affected (Table 1). Nucleotide sequence analysis of selected mutant RS junctions confirmed the presence of deletions, some as great as 20 bp (Fig. 2B). The recovery of recombinant plasmids in this assay depends on the integrity of the gene that encodes chloramphenicol acetyl transferase; consequently, deletions larger than 350 bp are not detected (Fig. 2A). To determine whether larger deletions are generated, we examined substrates recovered from XR-1 cells that confer ampicillin resistance but fail to hybridize to a probe for the sequence (OOP) normally deleted by V(D)J recombination (Fig. 2A). Two such recombinants, which contained deletions of about 2 and 4 kb, were detected from 600 screened colonies (0.3%). Thus, a substantial number of abnormally large deletions occur but are not identified in the double selection procedure. Similarly, an analysis of coding junctions showed that these, too, had abnormally large deletions, although some recombination points were within the normal range (Fig. 3B).

To compare the manifestations of the homozygous *scid* mutation to those of the two x-ray–sensitive CHO lines, we assayed *scid* fibroblasts by the transient V(D)J recombination assay. As observed previously

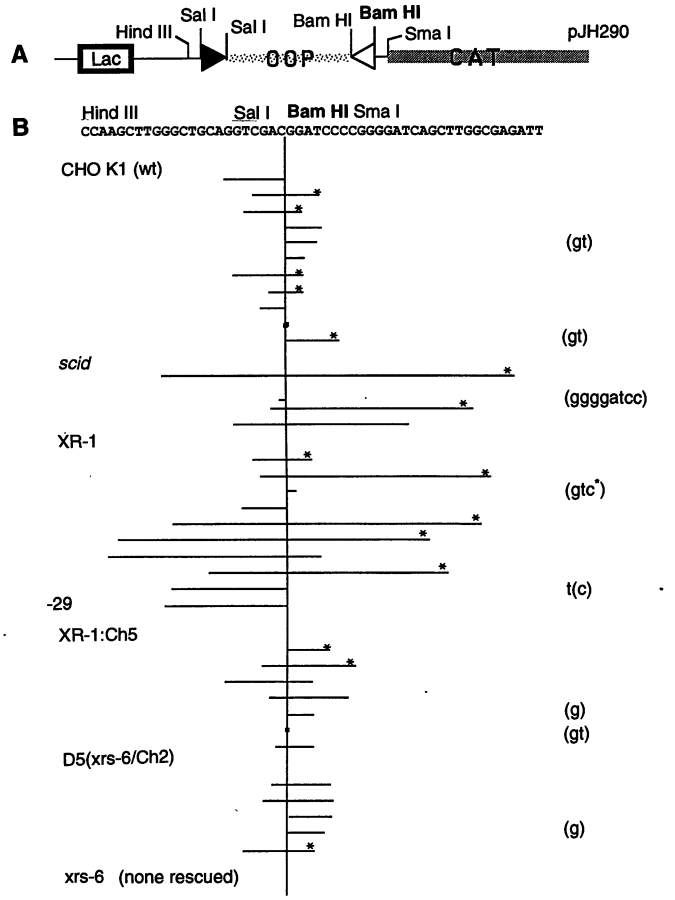


**Fig. 3.** Nucleotide sequence analysis of random coding joins. (**A**) Map of the pJH290 (*6*) region that contains the RS sequences; details are as described in Fig. 2. (**B**) The nucleotide sequence represents the product of a coding join in which no nucleotides have been lost. The solid lines below represent the extent of deletions in coding joins isolated from substrates recovered from the indicated cell lines. Asterisks represent bases that could not be assigned unequivocally. Bases inserted at the joins are listed at the right of the figure in lowercase letters; all except one of these (not in parentheses) are consistent with P elements (*14*). The short sizes of the P elements in the XR-1 joins are consistent with those found in normal cells, whereas *scid* cells often have much larger P elements (*23*).

**Table 1.** Analysis of signal and coding joins formation in CHO cell lines by transient V(D)J recombination assay (*9*). Abbreviations are as follows: wt, wild type; ND, not determined; NA, not applicable; S, sensitive; P, partial; L, low cross-sensitivity; and (−), indistinguishable from wild type.

| Cell line | Sensitivity | | pJH200 (signal) | | pJH290 (coding) | | Correct joins (%)* |
|---|---|---|---|---|---|---|---|
| | UV | X-ray | $Amp^RCam^R/Amp^R$ | Percent | $Amp^RCam^R/Amp^R$ | Percent | |
| AA8 (wt) | — | — | (240/5950) | 4.0 | (127/1825) | 6.9 | 99 |
| Mock | — | — | (2/3600) | 0.05 | (22/30225) | 0.07 | NA |
| UV5 | S | — | (140/6375) | 2.0 | (87/2025) | 4.3 | 99 |
| UV20 | S | — | (630/11390) | 5.7 | (152/1315) | 12.0 | 97 |
| EM9 | S | L | (80/1950) | 4.0 | (140/2700) | 5.1 | 99 |
| UV24 | S | — | (1000/26350) | 3.8 | (230/2585) | 8.8 | 97 |
| UV135 | S | — | (133/1955) | 6.8 | (106/970) | 11.0 | 98 |
| UV61 | S | — | | ND | (165/2935) | 5.6 | ND |
| UV41 | S | — | (145/1580) | 9.0 | (94/1040) | 9.0 | ND |
| K1 (wt) | — | — | (155/6800) | 2.3 | (170/9310) | 1.8 | 99 |
| Mock | — | — | (—/5775) | <0.01 | | ND | NA |
| xrs-6 | — | S | (117/96000) | 0.10 | (83/504000) | 0.02 | 14 |
| xrs-6Rev (*24*) | — | I | (64/8800) | 0.7 | (24/3255) | 0.75 | 99 |
| xrs-6/Ch2(D5) (*24*) | — | I | (198/14450) | 1.4 | (70/8850) | 0.8 | 99 |
| 4362A (wt) | — | - | (131/12320) | 1.0 | (70/6880) | 0.92 | 99 |
| Mock | — | - | (—/2272) | <0.04 | | ND | NA |
| XR-1 | — | S | (272/258400) | 0.10 | (153/540800) | 0.02 | 10 |
| XR-1:Ch5 (*24*) | — | — | (54/1804) | 3.0 | (28/1309) | 2.1 | 99 |
| XR-1/xrs-6 (*24*) | — | — | (135/5040) | 2.6 | (47/3645) | 1.3 | 99 |
| K1 (wt) | — | — | (155/2850) | 5.4 | (262/2800) | 9.3 | 99 |
| Mock | — | — | (—/8960) | <0.01 | | ND | NA |
| BLM-1 | — | S | (500/10000) | 5.0 | (>400/10000) | >4.0 | 99 |
| BLM-2 | S | S | (>300/10000) | >3.0 | (>300/10000) | >3.0 | 99 |
| ADR-3 | — | S | (98/1900) | 5.0 | (166/1088) | 10.0 | 99 |
| *scid* (SCGR11) | — | S | (40/710) | 5.6 | (38/13280) | 0.30 | 80 |
| *scid*/xrs-6 (*24*) | — | — | (71/2352) | 3.1 | (130/3056) | 4.2 | 80 |

*Percentage of correct RS joins screened by digestion of the PCR products of the recombinant substrate pJH200 with Hgi AI (see Fig. 2).

(*13*), the *scid* fibroblasts had impaired coding join formation but, unlike xrs-6 and XR-1 cells, had a relatively normal level and fidelity (80% precise) of RS joins (Table 1). This finding suggested that the *scid* mutation affects a different gene than the xrs-6 and XR-1 mutations. To verify this conclusion, we made multiple cell hybrids between these lines and found a complete complementation of radiation sensitivity. Furthermore, V(D)J recombination activity was restored to normal in the one hybrid (xrs-6/*scid*) tested (Table 1). We conclude that xrs-6, XR-1, and *scid* represent three different genes involved in V(D)J recombination.

The xrs-6 and XR-1 mutations affect both RS and coding join formation (Fig. 1E); however, recognition and introduction of double-strand breaks appear to occur normally in these mutants because some RS or coding joins have at least one end at or near the RS or coding junction, and recovered RS and coding joins linked sequences from the expected side of the involved elements. Therefore, it is likely that these mutations either result in hyperexonucleolytic activity or impair the normal joining process such that only illegitimate recombination events are recovered. The presence of extra nucleotides resembling normal P elements [(*14*) and Fig. 3] in the XR-1 mutant suggests that the defect in this mutant affects a V(D)J recombination step downstream of that involved in the generation of these elements and the activity affected by the *scid* defect (*13, 15*).

V(D)J recombination has some mechanistic similarities to certain transposition events. For example, P element transposition in *Drosophila* occurs by a cut-and-paste process usually followed by double-strand gap repair to restore the donor P element (*16*). A gene product (*mei-41*) necessary for recovery of P-bearing chromosomes undergoing transposition has also has been implicated in DSBR (*17*). Furthermore, protection of ends in DSB intermediates by a stable protein complex occurs in Tn7 and Tn10 transposition in *Escherichia coli* (*18*). In the radiosensitive Rad52 epistatis group of yeast, mutants show defects in meiotic and mitotic recombination (*19, 20*). Furthermore, yeast exhibit extensive exonucleolytic processing of broken DNA ends during meiosis and mating-type switching (*21*). In this context, the xrs-6 or XR-1 mutations might lead to a failure to protect free ends from extensive degradation by either the V(D)J complex or by normal cellular exonucleases.

## REFERENCES AND NOTES


1. F. W. Alt *et al.*, *Immunol. Today* **13**, 306 (1992).
2. D. G. Schatz, M. A. Oettinger, D. Baltimore, *Cell* **59**, 1035 (1989); M. A. Oettinger, D. G. Schatz, C. Gorka, D. Baltimore, *Science* **248**, 1517 (1990).
3. M. J. Bosma and A. M. Carroll, *Annu. Rev. Immunol.* **9**, 323 (1991).
4. B. A. Malynn *et al.*, *Cell* **54**, 453 (1988); M. R. Lieber *et al.*, *ibid.* **55**, 7 (1988); T. K. Blackwell *et al.*, *EMBO J.* **8**, 735 (1989).
5. G. M. Fulop and R. A. Phillips, *Nature* **347**, 479 (1990); K. A. Biedermann *et al.*, *Proc. Natl. Acad. Sci. U.S.A.* **88**, 1394 (1991); E. A. Hendrickson *et al.*, *ibid.*, p. 4061.
6. J. E. Hesse, M. R. Lieber, M. Gellert, K. Mizuuchi, *Cell* **49**, 775 (1987).
7. One microgram of the corresponding recombination substrates pJH200 or pJH290 (*6*) was cotransfected with 3 μg of each of the genomic expression vectors RAG-1 and RAG-2 under the control of the RSV-LTR promoter (*1*) with the use of standard $CaPO_4$ method. Mock transfections were performed in the corresponding wild-type cell line transfected only with the recombination substrate. This transient assay procedure to test for ability to rearrange introduced V(D)J recombination substrates has been described (*6*).
8. J. H. J. Hoeijmakers and D. Bootsma, *Cancer Cells* **2**, 311 (1990).
9. P. A. Jeggo, *Mutat. Res.* **239**, 1 (1990).
10. C. N. Robson, A. L. Harris, I. D. Hickson, *ibid.* **217**, 93 (1989).
11. P. A. Jeggo *et al.*, *Proc. Natl. Acad. Sci. U.S.A.* **89**, 6423 (1992).
12. A. J. Giaccia *et al.*, *Am. J. Hum. Genet.* **747**, 459 (1990).
13. M. A. Lieber, *FASEB J.* **5**, 2934 (1991).
14. J. J. Lafaille *et al.*, *Cell* **59**, 859 (1989).
15. D. B. Roth *et al.*, *ibid.* **70**, 1 (1992).
16. W. R. Engels, D. M. Johnson-Schlitz, W. B. Eggleston, J. Sved, *ibid.* **62**, 515 (1990).
17. S. S. Banga, A. Velazquez, J. B. Boyd, *Mutat. Res.* **255**, 79 (1991).
18. R. Bainton, P. Games, N. L. Craig, *Cell* **65**, 805 (1991); D. B. Haniford, H. W. Benjamin, N. Kleckner, *ibid.* **64**, 171 (1991).
19. A. Shinohara, H. Ogawa, T. Ogawa, *ibid.* **69**, 457 (1992).
20. E. C. Friedberg, *Microbiol. Rev.* **52**, 70 (1988).
21. L. Cao, E. Alani, N. Kleckner, *Cell* **61**, 1089 (1990).
22. The RS joins from recovered plasmids were amplified by PCR with the primers 5′-CTTTCATTGCCATACG-3′ and 5′-AGCGGATAACAATTTCACACAGGA-3′. Twenty-five cycles of amplification were performed in 50 μl of 10 mM tris-HCl (pH 8.3), 50 mM KCl, 1.5 mM $MgCl_2$, 0.01% (w/v) gelatin, and 50 ng of each primer plus 1.0 U of Taq polymerase (Perkin-Elmer). Denaturation was at 94°C for 45 s, annealing was at 52°C for 1 min, and elongation was at 72°C for 3 min. The PCR product was digested with Hind III and size-separated by electrophoresis on a 2.5% agarose gel. Precise V(D)J recombination generates a 150-bp band that contains the RS without the 200-bp OOP sequence. Alkaline-lysed minipreps were prepared and sequenced with a Sequenase kit (United States Biochemical Corp.) according to the manufacturer's instructions.
23. W. Schuler, N. R. Ruetsch, M. Amsler, M. J. Bosma, *Eur. J. Immunol.* **21**, 589 (1991); L. Kienker, W. A. Kuziel, P. W. Tucker, *J. Exp. Med.* **174**, 769 (1991).
24. The xrs-6Rev and xrs-6/Ch2(D5) are xrs-6 cells that have been reactivated after treatment with azacytidine (*9*) or complemented by the presence of human chromosome 2 (*11*), respectively. XR-1:Ch5 is the corresponding hybrid containing human chromosome 5 that fully complements the DSBR defect (*12*). The *scid*/xrs-6 and XR-1/xrs-6 are the two different kind of hybrids generated by cell fusion as described elsewhere (*9*). The results presented for the xrs-6 and XR-1 mutants plus the complemented derivatives of these lines were reproduced in at least three independent transfection experiments.
25. The UV-sensitive cell lines (UV and EM9) were provided by L. Thompson. The *scid* fibroblast cell line SCGR11 was provided by D. Weaver. The bleomycin (BLM-1 and BLM-2)- and adryamicin (ADR-3)-resistant CHO cell lines were provided by I. Hickson and C. Robson. The substrates pJH200 and pJH290 were provided by J. Hesse and M. Gellert. Supported by NIH grant A.I. 20047 (to F.W.A.); the Howard Hughes Medical Institute, EC contract B17-0026 (to P.A.J.); NIH grant CA45277 (to T.S.); and postdoctoral fellowships from the Irvington Institute (to G.E.T.) and the Cancer Research Institute (to E.O.).


6 November 1992; accepted 11 January 1993

# Evolution of Endothermy in Fish: Mapping Physiological Traits on a Molecular Phylogeny

Barbara A. Block,* John R. Finnerty, Alexandre F. R. Stewart, Jessica Kidd

**Mackerels, tunas, and billfishes (suborder Scombroidei and Teleostei) provide an ideal taxonomic context in which to examine the evolution of endothermy. Multiple origins and diverse strategies for endothermy exist among these fish. Here a molecular phylogeny of the Scombroidei has been determined by direct sequencing of a portion of the mitochondrial *cytochrome b* gene. The distribution of endothermic species within this proposed genealogy indicates that the ability to warm the brain and retina arose independently in three lineages, each time in association with a movement into colder water. This suggests that the evolution of cranial endothermy in fish was selected in order to permit thermal niche expansion and not selected for increased aerobic capacity.**

The majority of the 30,000 species of teleost fishes are ectotherms with body temperatures within 1° to 2°C of ambient water temperature. Endothermy, the ability to maintain elevated body temperature by metabolic means, has been documented only within one major assemblage of large oceanic teleosts, the Scombroidei (*1–3*). Sharks of the family Lamnidae and Alopiidae have convergently evolved endothermy (*3, 4*). The transition from ectothermy to endothermy requires the elevation of aerobic capacity (and hence heat production) and the reduction of the rate of

Department of Organismal Biology and Anatomy, University of Chicago, Chicago, IL 60637.

*To whom correspondence should be addressed.